Physical Science International Journal
6(1): 26-34, 2015, Article no.PSIJ.2015.030
ISSN: 2348-0130

SCIENCEDOMAIN *international*
www.sciencedomain.org

The Optical-Electro-Chemical Properties of CdS/CdSe/ZnS Co-Sensitized TiO_2 Solar Cells

H. T. Tung[1*]

[1]*Faculty of physics, Dong Thap University, Dong Thap Province, Vietnam.*

Author's contribution

The sole author designed, analyzed and interpreted and prepared the manuscript.

Article Information

DOI: 10.9734/PSIJ/2015/15227
Editor(s):
(1) B. Boyacioglu, Vocational School of Health, Ankara University, Kecioren, Ankara, Turkey.
(2) Christian Brosseau, Distinguished Professor, Department of Physics, Université de Bretagne Occidentale, France.
Reviewers:
(1) Anonymous, Taiwan.
(2) Anonymous, Turkey.
Complete Peer review History: http://www.sciencedomain.org/review-history.php?iid=836&id=33&aid=7798

Original Research Article

Received 14th November 2014
Accepted 17th December 2014
Published 15th January 2015

ABSTRACT

Quantum dots solar cells (QDSSCs) based on the different CdS/CdSe/ZnS-TiO_2 photo anodes were prepared by successive ionic layer adsorption and reaction (SILAR) processes. The CdS, CdSe and ZnS layers were considered by UV–Vis spectra for optical and the SILAR cycles of CdS, CdSe and ZnS show different impact on the performance of QDSSCs. With the deposition times of CdS increasing (from 1 to 5 cycles), the short circuit current density of the device is enhanced. On the contrary, the increasing deposition times of CdSe (from 1 to 5 cycles) has a negative effect for the generation and collection of photoelectron. In addition, the electrochemical impedance spectroscopy technology (EIS) was used to investigate the diffusion and recombination in QDSSCs. In addition, the dynamic resistances were discussed based on the EIS results.

Keywords: Quantum dots; solar cells; photo anodes.

1. INTRODUCTION

Quantum dot-sensitized solar cells (QDSSCs) are considered as a promising low-cost alternative for third generation photovoltaic [1]. This solar cell is sourcing from the dye-sensitized solar cell (DSSC), which is based on sandwich dye-sensitized nanocrystalline work electrode, counter-electrode and electrolyte. Compared to the conversional DSSC, the sensitizer of QDSSC is replaced by semiconductor quantum dots (QDs) such as CdS [2], PbS [3], Ag_2S [4], CdSe

**Corresponding author: Email: tunghtvlcrdt@gmail.com;*

[5], Ag_2Se [6], CdTe [7] and InAs [8] which possess multiple advantages as tunable band gaps, high extinction coefficient, and high photo stability [9-11]. Unfortunately, QDSSC which promises a high theoretical efficiency up to 44% for its special multi electrons generation character [12], still presents lower energy conversion efficiency and far below the theoretical value. For QD-sensitizers, CdS, CdSe and ZnS have been paid much attention because of their high potential in photo absorption under visible region. The two materials exhibit different characteristics. For CdS, its conduction band (CB) edge is higher than that of TiO_2, making the electron injection from CdS to TiO_2 very effective, but the absorption range of CdS is too narrow, which restrict the utilization of light. Lee and Lo [13], model system prepared by SILAR is favorable than single CdS or CdSe, which can extend spectral response to the visible light region and charge injection from QDs to TiO_2. The influence of SILAR cycles on the performance has also been investigated recently [14]. However, the detailed optical and especially electrochemical properties of the photo anodes with different SILAR cycles are still lack of deep research. In this paper, we prepared CdS/CdSe/ZnS co-sensitizer on meso porous TiO_2 surfaces with different SILAR cycles. The optical properties of the photo anodes and the photovoltaic performance of the corresponding solar cells were investigated. Moreover, EIS was employed to investigate the interface impedance and chemical capacitance of QDSSCs. Based on the EIS results, the SILAR deposition cycles effect on the charge recombination was discussed.

2. EXPERIMENT

2.1 Materials

$Cd(CH_3COO)_2.2H_2O$ (99%), KCl, Na_2S, $Zn(NO_3)_2$, Se powder, S powder, Na_2SO_3, $TiCl_4$, TiO_2 paste obtained from Dyesol, Australia.

To prepare TiO_2 films, the TiO_2 thin films were fabricated by silk-screen printing with commercial TiO_2 paste. Their sizes ranged from 10 to 20 nm. Two layes of film with thickness of 8 μm (measured by microscope). Then, the TiO_2 film was heated at 400ºC for 5 min, 500ºC for 30 min. Afterward, the film was dipped in 40-mmol $TiCl_4$ solution for 30 min at 70ºC and heated at 500ºC for 30 min. The specific surface area of the mesoporous TiO_2 were investigated by using the N_2 adsorption and desorption isotherms before and after the calcination. The surface area is 120.6 m^2g^{-1} (measured by BET devices). This result indicates that the synthesized material has wider mesoporous structure.

To prepare TiO_2/CdS/CdSe/ZnS films,the highly ordered TiO_2 were sequentially sensitized with CdS, CdSe and ZnS QDs by SILAR method. First, the TiO_2 film was dipped in 0.5 mol/L $Cd(CH_3COO)_2$-ethanol solution for 5 min, rinsed with ethanol, dipped for 5 min in 0.5 mol/L Na_2S-methanol solution and then rinsed with methanol. The two-step dipping procedure corresponded to one SILAR cycle and the incorporated amount of CdS QDs was increased by repeating the assembly cycles for a total of three cycles. For the subsequent SILAR process of CdSe QDs, aqueous Se solution was prepared by mixing Se powder and Na_2SO_3 in 50ml pure water, after adding 1 mol/L NaOH at 70ºC for 7h. The TiO_2/CdS samples were dipped into 0.5 mol/L $Cd(CH_3COO)_2$-ethanol solution for 5 min at room temperature, rinsed with ethanol, dipped in aqueous Se solution for 5 min at 50ºC, rinsed with pure water. The two-step dipping procedure corresponds to one SILAR cycle. Repeating the SILAR cycle increases the amount of CdSe QDs (a total of four cycles). The SILAR method was also used to deposit the ZnS passivation layer. The TiO_2/CdS/CdSe samples were coated with ZnS by alternately dipping the samples in 0.1 mol/L $Zn(NO_3)_2$ and 0.1 mol/L Na_2S-solutions for 5 min/dip, rinsing with pure water between dips (a total of two cycles). Finally, it was heated in a vacuum environment with different temperatures to avoid oxidation (Fig. 1). The TiO_2/CdS/CdSe/ZnS was be measured thickness by microscopic. The results of the average thickness of CdS(1), CdSe(1), ZnS(1) are 40 nm, 43.3 nm, 40 nm respectively.

2.2 Fabrication of QDSSCs

The polysulfide electrolyte used in this work was prepared freshly by dissolving 0.5 M Na_2S, 0.2 M S, and 0.2 M KCl in Milli-Q ultrapure water/methanol (7:3 by volume). The CdS/CdSe/ZnS co-sensitized TiO_2 photoanode and Pt counter electrode were assembled into a sandwich cell by heating with a Surlyn. The electrolyte was filled from a hole made on the counter electrode, which was later sealed by thermal adhesive film and a cover glass. The active area of QDSSC was 0.38 cm^2.

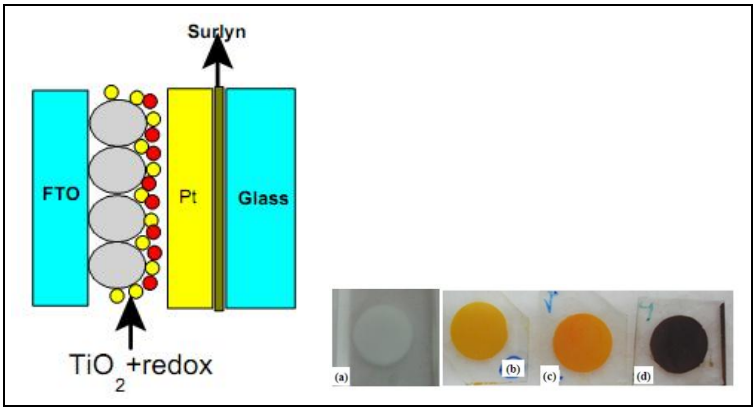

Fig. 1. The diagram shows the instruction of the QDSSCs and images of photo anodes

2.3 Characterizations and measurements

The morphology of the prepared samples was observed using fieldemission scanning electron microscopy FE-SEM, S4800). The crystal structure was analyzed by an X-ray diffractometer (XRD) with CuKα radiation. The absorption properties of the samples were investigated by UV–vis spectrum (JASCO V-670). Photocurrent – Voltage measurements were performed on a Keithley 2400 sourcemeter using a simulated AM 1.5 sunlight with an output power of 100 mW/cm^2 produced by a solar simulator (Solarena, Sweden).

3. RESULTS AND DISCUSSION

Detailed morphological features and crystal of the pure TiO_2 and TiO_2/CdS/CdSe/ZnS photo anodes were investigated using TEM image. A typical TEM image of pure TiO_2 film is depicted in Fig. 2a. It is quite evident that the mean diameter of TiO_2 nanoparticle is about 25 nm. Fig. 2b shows a TEM image of the TiO_2/CdS/CdSe/ZnS photo anode prepared with the SILAR cycle number of CdS, CdSe and ZnS at 3, 3 and 2. We can clearly see that QDs uniformly cover the surface of TiO_2 nanoparticles. It shows that the average diameter of QDs is from 2 nm to 3 nm. The results of the TEM demonstrate that the SILAR method is an efficient TiO_2 sensitization strategy for obtaining well covering the QDs on the TiO_2 surfaces.

The optical performance of co-sensitized TiO_2 thin films can be monitored by studying the absorbance and energy band gap of the materials. Fig. 3a shows the UV–Vis spectrum of thus sensitized electrodes measured after each cycle of SILAR. As expected, the absorbance increased with the deposition cycles of CdS, CdSe and ZnS. However, only absorption spectra with SILAR cycles of the electrode TiO_2/CdS(3)/CdSe(3)/ZnS(2) obtains the best efficiency as discussed in the following section. The change of absorbance is due to QDs that was loaded on TiO_2 film. Moreover, the increasing successive deposition cycles also caused a red shift of UV-Visthat lossesby quantum confinement effect [15]. The average sizes of CdS, CdSe and ZnS are consistent with the FE-SEM images. The effect of deposition cycles of CdS, CdSe and ZnS can be clearly seen on the energy band gap values of CdS/CdSe/ZnS co-sensitized TiO_2 films. The estimated band gaps vary from 1.97 eV to 2.7 eV, which are higher than the values reported for CdS and CdSe in bulk (2.25 eV and 1.7 eV [1], respectively), indicating that the sizes of CdS, CdSe and ZnS on TiO_2 films are still within the scale of QDs. A higher absorption is thus obtained because the absorption spectrum of ZnS complements those of the CdSe and CdS QDs. Furthermore, ZnS acts as a passivation layer to protect the CdS and CdSe QDs from photo corrosion [16]. Fig. 3b shows the PL of different photoanodes that their thick is changed by the cycles SILAR. After the CdS, CdSe, and ZnS QDs are sequentially deposited onto the TiO_2 film, a cascade type of energy band structure is constructed for the co-sensitized photo anode. The best electron transport path is from the CB of ZnS and CdSe to that of CdS, and finally, to TiO_2 film (shows Fig. 6b). Thus, the PL of TiO_2/CdS/CdSe/ZnS was quenched (displayed in Fig. 3b). This reveal that TiO_2 film serve as effective quenchers of excited CdS, CdSe and ZnS QDs. The thick photo anode film quenches more efficiently than thin photo anode film.

The structure of the TiO_2/QDs photo electrodes for photovoltaic applications, shown in Fig. 4(a), are studied by the XRD patterns. It reveals that the TiO_2 have a Anatase structure with a strong (101) peak located at 25.4º, which indicates that the TiO_2 film are well crystallized and grow along the [101] direction. Three peaks can be observed at 26.4º, 44º and 51.6º, which can be indexed to (111), (220) and (331) of cubic CdS, CdSe respectively. Two peaks can be observed at 48º and 54.6º, which can be indexed to (220) and (331) of cubic ZnS respectively. It demonstrates that the QDs have crystallized onto the TiO_2 film. Fig. 4(b) is the Raman spectrum of the TiO_2/QDs photo electrodes. It shows that an anatase structure of the TiO_2 films have five oscillation modes correspond to wave number at 143, 201, 395, 515 and 636 cm^{-1}. In addition, two peaks can be observed at 201, 395, and 515 cm^{-1}, which can be indexed to the cubic structure of CdS, CdSe. The results of the Raman is likely the results of XRD. Fig. 4(b) is the energy dispersive X ray spectrum of the TiO_2/CdS/CdSe/ZnS film. It shows that the Ti and O peaks are from the TiO_2 film, Cd, Se, Zn and S peaks, clearly visible in the EDS spectrum, are from the QDs. The Si is from the FTO and C is from the solvent organic. That shows, the QDs are well deposited onto the TiO_2.

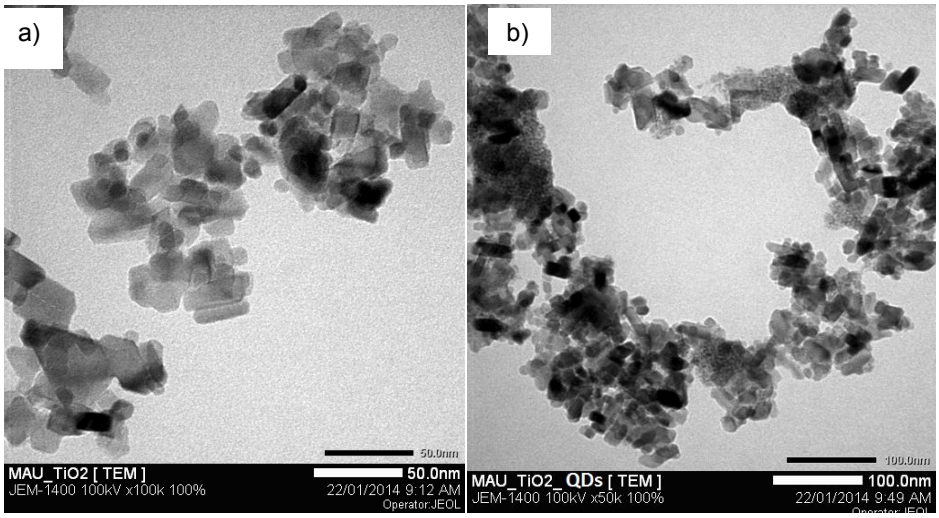

Fig. 2. TEM images of (a) TiO_2 film and (b) TiO_2/CdS/CdSe/ZnS film

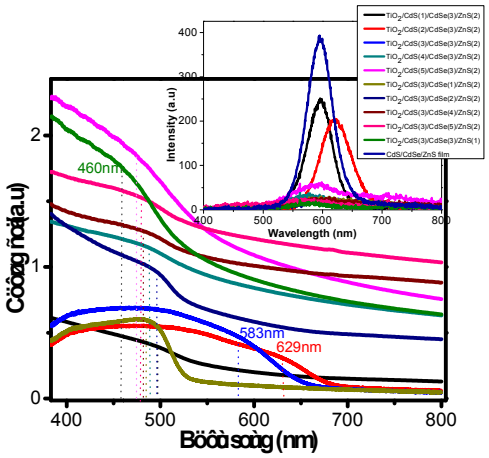

Fig. 3. UV–Vis absorption spectra of the TiO_2 films sensitized by CdS/CdSe/ZnS QDs shows the light absorption behavior of photoanodes changed with the SILAR cycles of CdS, CdSe and ZnS and Photoluminescence (PL) spectra of the TiO_2/CdS/CdSe/ZnS (small image)

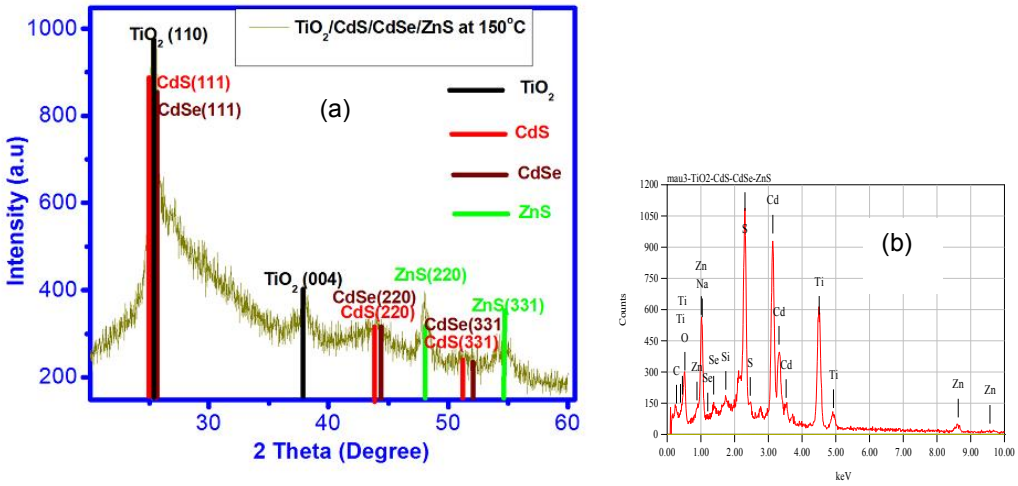

Fig. 4. (a) XRD and (b) Energy dispersive X - ray spectrum (EDS) of TiO_2/CdS/CdSe/ZnS photo anodes

In order to understand the effects of SILAR cycles of CdS, CdSe and ZnS, we prepared a series of combinations of CdS, CdSe and ZnS QDs on TiO_2 films, investigated their photovoltaic performances with polysulfide electrolyte. All the samples were coated with ZnS to inhibit the recombination at the TiO_2 photo anode/polysulfide electrolyte interface [17]. Table 1 presents the photocurrent density voltage characteristics of the QDSSCs with different CdS/CdSe/ZnS co-sensitized TiO_2 films (active area of 0.38 cm^2) at AM 1.5 (100 mW/cm^2), and the related parameters of these QDSSCs are listed in Table 1. It shows that the power conversion efficiencies of QDSSCs are increasing with the SILAR cycle number of CdS, CdSe and ZnS at 3, 3 and 2, respectively. It is noted that lower power conversion efficiency was obtained for those cells with either less CdS and CdSe SILAR cycles than 3 or more CdS and CdSe SILAR cycles than 3 (shows Fig 5b). QDSSCs based on the TiO_2/CdS(3)/CdSe(3)/ZnS(2) photo anode shows an open-circuit voltage (V_{oc}) of 0.76 V, a short-circuit current density (J_{sc}) of 4.79 mA/cm^2, fill factor (FF) of 0.41 and an energy conversion efficiency (**η**) of 1.52%. As the deposition cycles of CdS and CdSe increase, there were slightly changes in V_{oc} and FF values. Besides, the J_{sc} decreases which cause in a reduced**η** (from 1.52% to 0.45%). These results indicate that better light absorption performance were obtained while more CdSe loaded on TiO_2/CdS. However, TiO_2/CdS/Cd Sephotoanode can increase recombination in QDSSCs. On the contrary, the increase of ZnS leads to the increasing generation of photoelectron and is helpful to collect excited electrons from ZnS, CdSe and CdS to TiO_2 film.

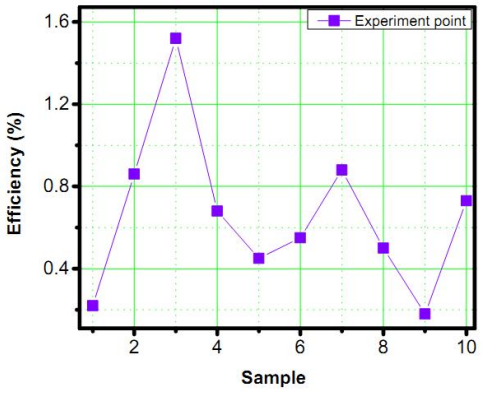

Fig. 5. Diagram shows the values efficiency of solar cells

J_{SC} is given by equation:

$$J_{SC} = q \int b_s(E) QE(E) dE \qquad (1)$$

J_{SC} is the photon current density and $b_s(E)$ is the number of photon the range EtoE+dEper unit are aper unit time. q is the charge of the electron, QE depends on the absorption coefficient of the materialsolar cell. The short-circuit current depends on a number of factors: the area of the solar cell, the number of photons, the spectrum of the incident light, the optical properties (absorption and reflection) and the collection probability of the solar cell, which depends

chiefly on the surface passivation and the minority carrier lifetime in the base. From Equation1, we see that the J_{SC} is not directly dependent on the thickness of the layer of QDs. When the thickness of the layer of QDs changes, the results change the absorption spectrum and the collection probability of the solar cell. After all, they cause change of J_{SC}, however, this change is nonlinear.

An equation for V_{oc} is found by setting the net current equal to zero in the solar cell equation to give:

$$V_{OC} = \frac{kT}{q} ln\left(\frac{I_L}{I_o} + 1\right) \quad (2)$$

The above equation shows that V_{oc} depends on the saturation current of the solar cell and the light-generated current. The saturation current, I_0 depends on recombination in the solar cell. Open-circuit voltage is then a measure of the amount of recombination in solar cells. FF depend on V_{OC} values, the junction quality (related with the series R_s) and the type of recombination in a solar cell. From Table 1, V_{OC} values change according to the film thickness from 0.29 to 0.76, corresponding to the change in FF from 0.26 to 0.41. Therefore the FF is the low value because V_{OC} is low. On the other hand, V_{OC} depend on the recombination process, particularly they are large, it gives low open-circuit voltages. In addition, FF is effected by R_s. The equations of R_s can be calculated by Thongpron and co-workers [18].

$$R_s = \frac{V_1 - V_2}{I_2 - I_1} - \frac{1}{\lambda(I_2 - I_1)} \ln[\frac{I_{ph} + I_o - I_1}{I_{ph} + I_o - I_2}] \quad (3)$$

Two operating points (I_1, V_1) and (I_2, V_2) on a single I-V curve. $\lambda = \frac{q}{nKT}$; I_{ph}, I_o are the photocurrent and the diode reverse saturation current. R_s values are calculated from 55 to 158 $m\Omega cm^{2-}$. This values is large as result as low FF.

QDSSCs based on TiO_2/CdS/Cdse/ZnSphoto anode have obtained a better efficiency than both QDSSCs based on TiO_2/CdS and TiO_2/Cd Sephoto anodes [19]. The result shows that the excited electrons have injected from conduction band (CB) of CdSe QDs to CB of TiO_2in which they may not be effective because of the quasi Fermi levels (E_F) of CdSe being lower than that of TiO_2 [13]. On the other hand, the E_F of CdSQDs is higher than that of the TiO_2 [20], so it have improved the electrons injection from CdSe to TiO_2. In addition, a Zn Slayer was coating to forms a potential barrier between the QDs and the electrolyte, which blocks the electrons in the CB from recombination with the electrolyte [21]. Resulting in a high performance of efficiency. Because the E_F of CdS is higher than of TiO_2, beneficial effects are conferred to the coupled QDSSC system. From Table 1, it is evident that the photocurrent density of the coupled QDSSC was influenced by CdS/CdSe/ZnS co-sensitization cycles [22], which can be explained in two ways. Firstly, particle size variation in CdS, CdSe and ZnS QDs leads to E_F alignment and consequently, so the CB of of CdS, CdSe, ZnS is higher that of TiO_2. As result, the excited electrons were transferred in TiO_2 easier [23].

In order to research the dynamic processes in the QDSSCs, we have measured EIS plot under dark conditions at varying negative applied bias (0.7–0 V). Fig. 6a shows the Nyquist plots of the CdS(3)/CdSe(3)/ZnS(2) QDs - sensitized solar cells. There are two semicircles at nyquist at high frequency and low frequency. The small semicircle at high frequency corresponds to the resistance movement of excited electrons at counter electrode/electrolyte (R_{ct1}) interface and FTO/TiO_2 interface. The large semicircle at low frequency from 10-100 kHz described resistance against the movement of excited electron in TiO_2 and recombination at TiO_2/QDs/electrolyte (R_{ct2}) interface and against inside the diffusion in electrolyte (Z_w). From Fig. 6a, we see that the 200Ω of R_{ct2} defined large, so it causes resistance the movement of electrons at the TiO_2/QDs/electrolyte interface and recombination of the electrons in polysulfide [22]. The Fig. 6b shows that the Bode plot with TiO_2/CdS(3)/CdSe(3)/ZnS(2) photo anode that is illuminated with an 1000W/m^2. At low frequency peaks corresponds to the movement of electrons at TiO_2/QDs/electrolyte interface, while the peak at higher frequencies describe the movement of electrons at the Pt/electrolyte interface. Lifetime of electrons in semiconductor (τ_e) is determined by the following formula = $1/2\pi f_{max}$. The f_{max} is the peak of the Bode plot at low frequencies, τ_e~3.2 ms.

Table 1. Photovoltaic performance parameters of QDSSCs based on different photo anodes

Samples	J_{SC} (mA/cm^2)	V_{OC}(V)	Fill factor FF	Efficiency η(%)
1	2.18	0.29	0.35	0.22
2	4.28	0.54	0.37	0.86
3	4.79	0.76	0.41	1.52
4	5.73	0.39	0.31	0.68
5	3.05	0.45	0.32	0.45
6	6.05	0.356	0.26	0.55
7	4.21	0.55	0.38	0.88
8	3.30	0.48	0.31	0.50
9	2.08	0.33	0.27	0.18
10	7.03	0.39	0.26	0.73

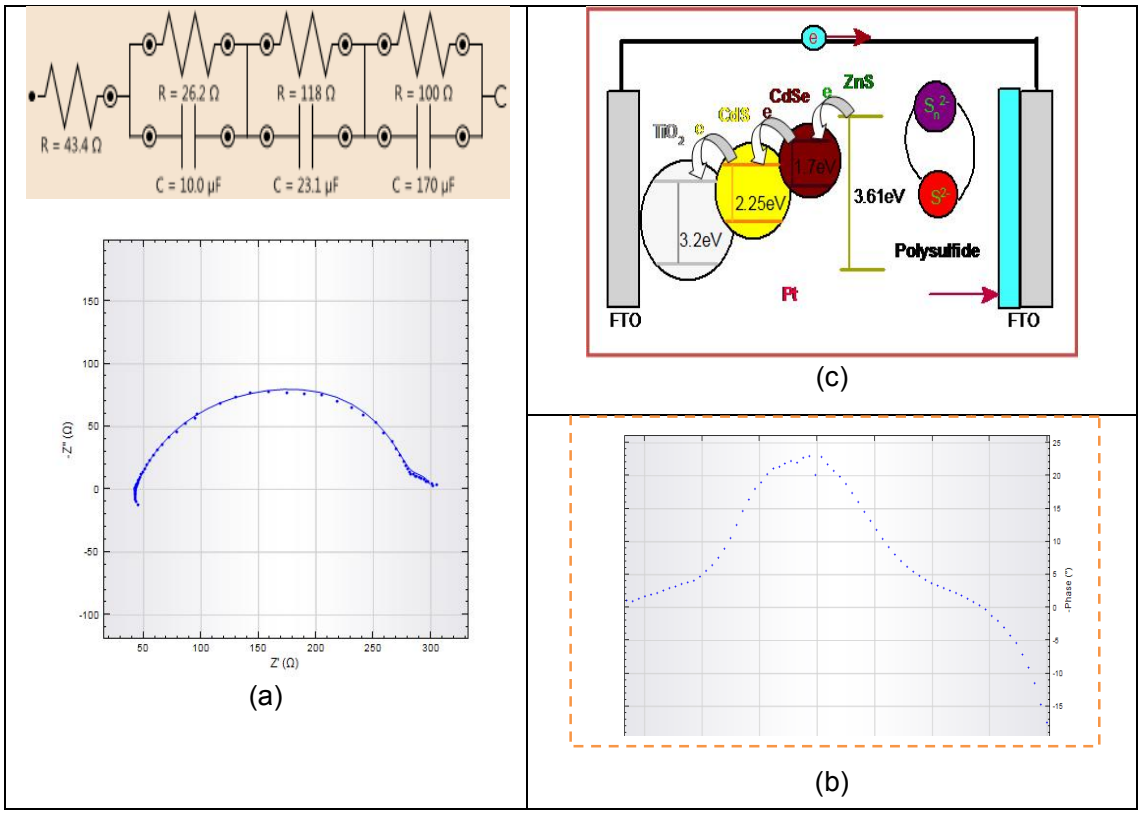

Fig. 6. (a) Nyquist plots of QDSSCs based on TiO_2/CdS(3)/CdSe(3)/ZnS(2) photo anode, (b) Bode plot and (c) the proposed energy band structure of QDSSCs[15].

4. CONCLUSIONS

We have successfully fabricate solar cells based on CdS/CdSe/ZnS- TiO_2 photo anodes which is researched the optical to depend on number of CdS, CdSe and ZnS SILAR cycles. With the deposition times of CdS increasing (from 1 to 5 cycles), the short circuit current density of the device is enhanced. On the contrary, the increasing deposition times of CdSe (from 1 to 5 cycles) has a negative effect for the generation and collection of photoelectron. For EIS spectrum, the SILAR deposition cycles effect on the charge recombination of excited electrons in TiO_2 and TiO_2/QDs interfaces. The synthesized TiO_2/CdS/CdSe/ZnS photo anode exhibits a maximum efficiency value of 1.52%.

COMPETING INTERESTS

Author has declared that no competing interests exist.

REFERENCES

1. Grätzel Michael. Photoelectrochemical cells. Nature 414.6861. 2001;338-344.
2. Wijayantha KGU, Peter LM, Otley LC. Fabrication of CdS quantum dot sensitized solar cells via a pressing route, Sol. Energy Mater. Sol. Cells. 2004;83:363.
3. Lee HJ, Leventis HC, Moon SJ, Chen P, Ito S, Haque SA, Torres T, Nüesch F, Geiger T, Zakeeruddin SM, Grätzel M, Nazeeruddin MK. Efficiency enhancement of solid-state PbS quantum dot-sensitized solar cells with Al_2O_3 barrier layer. Adv. Funct. Mater. 2009;19:2735.
4. Tubtimtae A, Wu KL, Tung HY, Lee MW, Wang GJ. Ag2S quantum dot-sensitized solar cells. Electrochem. Commun. 2010;12:1158.
5. Fuke N, Hoch LB, Koposov AY, Manner VW, Werder DJ, Fukui A, Koide N, Katayama H, Sykora M. CdSe quantum-dot sensitized solar cell with ~100% internal quantum efficiency. ACS Nano. 2010; 4: 6377.
6. Tubtimtae A, Lee MW,. Wang GJ. Ag2Se quantum-dot sensitized solar cells for full solar spectrum light harvesting. J. Power Sources. 2011;196:6603.
7. Bang JH, Kamat PV. Quantum Dot Sensitized Solar Cells. A Tale of Two Semiconductor Nanocrystals: CdSe and CdTe. ACS Nano. 2009;3:1467.
8. Yu PR, Zhu K, Norman AG, Ferrere S, Frank AJ, Nozik AJ. Nanocrystalline TiO2 solar cells sensitized with InAs quantum dots. J. Phys. Chem. 2006;B 110: 25451.
9. Gorer S, Hodes G. Quantum size effects in the study of chemical solution deposition mechanisms of semiconductor films. J. Phys. Chem. 1994;98:5338.
10. Moreels I, Lambert K, De Muynck D, Vanhaecke F, Poelman D, Martins JC, Allan G, Hens Z. Optical properties of zincblende cadmium selenide quantum dots. Chem. Mater. 2007;19:6101.
11. Nozik AJ. Multiple exciton generation in semiconductor quantum dots. J. Chem. Phys. Lett. 2008;457:3.
12. Hanna MC, Nozic AJJ. All chemically deposited, annealing and mesoporous metal oxide free CdSe solar cells. J. Appl. Phys. 2006;100:074510.
13. Lee YL, Lo YS. Highly Efficient Quantum-Dot-Sensitized Solar Cell Based on Co-Sensitization of CdS/CdSe. Adv. Funct. Mater. 2009;19:604
14. Gonzalez-Pedro V, Xu X, Mora-Sero I, Bisquert J. Modeling high-efficiency quantum dot sensitized solar cells. ACS Nano 2010;4:5783–90.
15. Pathan HM, Lokhande CD. Deposition of metal chalcogenide thin films by successive ionic layer adsorption and reaction (SILAR) method. Bulletin of Materials Science. 2004;27(2):85-111.
16. Tachan Z, Shalom M, Hod I, Ruhle S, Tirosh S, Zaban A. PbS as a highly catalytic counter electrode for polysulfide-based quantum dot solar cells. J. Phys. Chem. 2011;C 115:6162.
17. Lee YL, Lo YS. Highly efficient quantum-dot-sensitized solar cell based on co-sensitization of CdS/CdSe. Advanced Functional Materials. 2009;9:604–9.
18. Thongpron J, Kirtikara K, Jivacate C. A method for the determination of dynamic resistance of photovoltaic modules under illumination, Technical Digest of the 14th International Photovoltaic Science and Engineering Conference—PVSEC 14, 26–30 January 2004, Bangkok, Thailand; 2004.
19. Chang CH, Lee YL. Chemical bath deposition of CdS quantum dots onto mesoscopic TiO_2 films for application in quantum-dot-sensitized solar cells. Appl. Phys. Lett. 2007;91:053503.
20. Kim JY, Choi SB, Noh JH, Yoon SH, Lee SW, Noh TH, Frank AJ, Hong KS. Surfactant-assisted shape evolution of thermally synthesized TiO_2 nanocrystals and their applications to efficient photoelectrodes. Langmuir. 2009;25:5348.
21. Sudhagar P, Jung JH, Park S, Lee YG, Sathyamoorthy R, Kang YS, Ah H. The performance of coupled (CdS:CdSe) quantum dot-sensitized TiO_2 nanofibrous solar cells. Electrochemistry Communications. 2009;11:2220–2224.

22. Balisa N, Dracopoulosb V, Bourikasc K, Lianos P. Quantum dot sensitized solar cells based on an optimized combination of ZnS, CdS and CdSe with CoS and CuS counter electrodes. Electrochimica Acta. 2013;91:246–252.

23. Chris GV, Neugebauer J. Universal alignment of hydrogen levels in semiconductors, insulators and solutions. Nature. 2003;423:626.

Peer-review history:
The peer review history for this paper can be accessed here:
http://www.sciencedomain.org/review-history.php?iid=836&id=33&aid=7798